

pressure. The red solid residue was extracted with hexane (300 mL) and filtered. The volume of the filtrate was reduced to 100 mL and cooled to -20°C . Two crops of dark red crystals were collected by filtration. Yield: 11.6 g (65 %). M.p. $192-194^{\circ}\text{C}$; ^1H NMR (C_6D_6 , 30°C): $\delta = 29.7$ (4H, $\nu_{1/2} = 110$ Hz), 9.5 (36H, $\nu_{1/2} = 12$ Hz), -19.4 (18H, $\nu_{1/2} = 7$ Hz); elemental analysis (%) calcd for $\text{C}_{34}\text{H}_{58}\text{Cl}_2\text{U}$: C 52.7, H 7.48; found: C 52.6, H 7.55; EI MS: m/z : 774 [M^+]; the parent ion isotopic cluster was simulated: (calcd. %, obsvd. %): 774 (100, 100), 775 (38, 39), 776 (71, 71), 777 (25, 25), 778 (14, 14), 779 (5, 4).

2: THF (30 mL) was added to a mixture of KC_8 (140 mg, 1.04 mmol) and **1** (400 mg, 0.52 mmol). A dark green color was generated immediately in the solution upon the addition of solvent. The mixture was stirred for 2 h, after which a solution of pyridine *N*-oxide (100 mg, 1.05 mmol) in THF (25 mL) was added. The dark green color of the solution immediately turned dark reddish brown. The reaction mixture was stirred for 12 h, after which the solvent was removed under vacuum and the residue extracted with toluene and filtered through Celite. Dark reddish brown crystals of **2** were obtained from a cold (-30°C) concentrated toluene solution. Yield: 275 mg (54 %); IR (Nujol): $\tilde{\nu} = 690, 710\text{ cm}^{-1}$ (U–O); elemental analysis (%) calcd for $\text{C}_{109}\text{H}_{156}\text{N}_4\text{O}_{13}\text{U}_6$: C 41.45, H 4.98, N 1.77; found: C 41.91, H 5.40, N 1.53.

The magnetization of crystalline powdered samples of **2** was recorded between 5–300 K at 0.1 T with a SQUID magnetometer (Quantum Design). Values of the magnetic susceptibility were corrected for the underlying diamagnetic increment ($\chi_{\text{dia}} = -1660 \times 10^{-6}\text{ cm}^3\text{ mol}^{-1}$) by using tabulated Pascal constants and the effect of the blank sample holder (gelatine capsule/quartz wool).

Cyclic voltammetric studies were conducted by using a Perkin–Elmer Princeton Applied Research Corporation (PARC) Model 263 potentiostat under computer control using M270 software. Samples were run in 0.1 M tetrabutylammonium hexafluorophosphate solution in tetrahydrofuran at a platinum working electrode with a silver wire quasi-reference electrode in either a PARC microcell in the glove box or in a Schlenk cell. Measured potentials were calibrated by using the ferrocene/ferrocenium couple ($E_{1/2} \sim 0.55\text{ V}$ vs. NHE).

Received: April 23, 2001 [Z16983]

- [1] M. T. Pope, *Heteropoly and Isopoly Oxometalates*, Springer, Berlin, 1983.
 [2] V. W. Day, W. G. Klemperer, *Science* **1985**, 228, 4699.
 [3] *Chem. Rev.* **1998**, 98, 3–271.
 [4] W. N. Lipscomb, *Inorg. Chem.* **1965**, 4, 132.
 [5] G. Marcu, M. Rusu, D. Rusu, *J. Radioanal. Nucl. Chem.* **1999**, 242, 119.
 [6] K.-C. Kim, M. T. Pope, *J. Am. Chem. Soc.* **1999**, 121, 8512.
 [7] P. G. Allen, J. J. Bucher, D. L. Clark, N. M. Edelstein, S. A. Ekberg, J. W. Gohdes, E. A. Hudson, N. Koltsoyannis, W. W. Lukens, P. N. Neu, P. D. Palmer, T. Reich, D. K. Shuh, C. D. Tait, B. D. Zwick, *Inorg. Chem.* **1995**, 34, 4797.
 [8] B. J. Warner, B. L. Scott, C. J. Burns, *Angew. Chem.* **1998**, 110, 1005; *Angew. Chem. Int. Ed.* **1998**, 37, 959.
 [9] Crystallographic details for **2**: a dark red crystal ($0.12 \times 0.08 \times 0.04\text{ mm}$) was mounted from Paratone N oil onto a glass fiber and immediately placed on a Bruker P4/CCD/PC diffractometer. A hemisphere of data was collected by using a combination of ϕ and ω scans, with 30 second frame exposures and 0.3° frame widths. A total of 14413 reflections ($-14 \leq h \leq 15$, $-20 \leq k \leq 20$, $0 \leq l \leq 28$) were collected at $T = 203(2)\text{ K}$ in the θ range of $1.49-23.32^{\circ}$ of which 14413 were unique ($R_{\text{int}} = 0.0000$); $\text{MoK}\alpha$ radiation ($\lambda = 0.71073\text{ \AA}$). The structure was solved by using direct methods and difference Fourier techniques (SMART Version 4.210, Bruker Analytical X-ray Systems, Inc., 1996). All non-hydrogen anisotropic temperature factors were restrained by using the ISOR option, and hydrogen atoms were placed in calculated ($d_{\text{C-H}} = 0.96\text{ \AA}$ for methyl, 0.93 \AA for methyl) positions. The residual peak and hole electron density was 1.770 and -1.791 e \AA^{-3} . The absorption coefficient was 7.641 mm^{-1} . The least-squares refinement converged normally with residuals of $R1 = 0.0686$ ($I > 2\sigma(I)$), $wR2 = 0.1610$, and $\text{GOF} = 1.152$ (F^2); $\text{C}_{109}\text{H}_{156}\text{N}_4\text{O}_{13}\text{U}_6$, space group $P\bar{1}$ (no. 2), triclinic $a = 13.8298(7)$, $b = 18.681(1)$, $c = 25.335(2)\text{ \AA}$, $\alpha = 80.118(1)^{\circ}$, $\beta = 76.867(1)^{\circ}$, $\gamma = 72.803(1)^{\circ}$, $V = 6050.9(6)\text{ \AA}^3$, $Z = 2$, $F(000) = 2916$, $\rho_{\text{calcd}} = 1.733\text{ g cm}^{-3}$. Crystallo-

graphic data (excluding structure factors) for the structures reported in this paper have been deposited with the Cambridge Crystallographic Data Centre as supplementary publication no. CCDC-160613. Copies of the data can be obtained free of charge on application to CCDC, 12 Union Road, Cambridge CB21EZ, UK (fax: (+44) 1223-336-033; e-mail: deposit@ccdc.cam.ac.uk).

- [10] T. R. Mohs, G. P. A. Yap, A. L. Rheingold, E. A. Maatta, *Inorg. Chem.* **1995**, 34, 9.
 [11] J. B. Strong, G. P. A. Yap, R. Ostrander, L. M. Liable-Sands, A. L. Rheingold, R. Thouvenot, P. Gouzerh, E. A. Maatta, *J. Am. Chem. Soc.* **2000**, 122, 639.
 [12] G. K. Johnson, E. O. Schlemper, *J. Am. Chem. Soc.* **1978**, 100, 3645.
 [13] A. Müller, F. Peters, M. T. Pope, D. Gatteschi, *Chem. Rev.* **1998**, 98, 239.
 [14] M. S. Grigor'ev, N. A. Baturin, A. A. Bessonov, N. N. Krot, *Radiochemistry* **1995**, 37, 12.
 [15] I. A. Charushnikova, V. P. Perminov, S. B. Katser, *Radiochemistry* **1995**, 37, 454.
 [16] M. P. Wilkerson, C. J. Burns, H. J. Dewey, J. M. Martin, D. E. Morris, R. T. Paine, B. L. Scott, *Inorg. Chem.* **2000**, 39, 5277.
 [17] E. V. Dehmlow, C. Bollmann, *Z. Naturforsch. B* **1993**, 48, 457.

Rational Molecular Design and EPC Synthesis of a Type VI β -Turn Inducing Peptide Mimetic**

Tobias Hoffmann, Harald Lanig,* Reiner Waibel, and Peter Gmeiner*

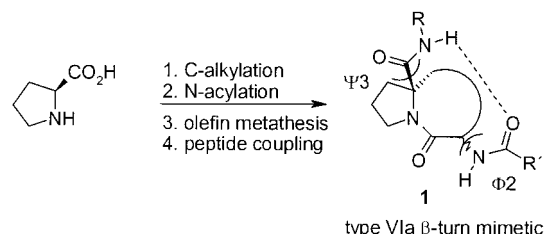
Besides the specific role of proline for the structure of proteins, experimental and simulation studies indicate that proline-containing sequence motives can act as molecular hinges, swivels, and switches and, thus, are involved in biological signaling processes.^[1] Furthermore, *cis/trans*-prolyl isomerization that can be catalyzed by rotamase enzymes is critical for the folding process.^[2] Recently, pseudoproline inducing a *cis*-peptide bond were introduced into the V3 loop of GP120 of HIV-1, which suggests that a *trans/cis* isomerization resulting in formation of a type VI β -turn conformation plays a crucial role in the infection process.^[3] Thus, the creation of type VI β -turn model systems is of interest for the discovery of molecular probes to gain detailed insight into the intermolecular interaction processes. Using appropriate con-

[*] Prof. Dr. P. Gmeiner, Dipl.-Chem. T. Hoffmann, Dr. R. Waibel
 Department of Medicinal Chemistry
 Emil Fischer Center, Friedrich-Alexander-University
 Schuhstrasse 19, 91052 Erlangen (Germany)
 Fax: (+49) 9131-85-22585
 E-mail: gmeiner@pharmazie.uni-erlangen.de
 Dr. H. Lanig
 Computer Chemistry Center
 Friedrich-Alexander-University
 Nögelsbachstrasse 25, 91052 Erlangen (Germany)
 Fax: (+49) 9131-85-26565
 E-mail: lanig@chemie.uni-erlangen.de

[**] This work was supported by the BMBF and the Fonds der Chemischen Industrie. EPC = enantiomerically pure compound.

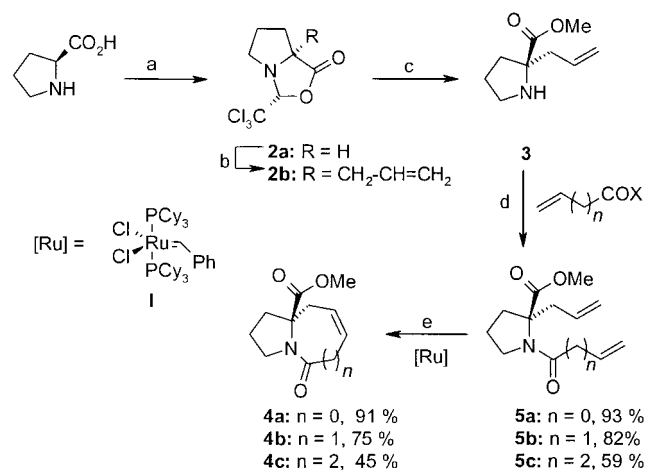
Supporting information for this article is available on the WWW under <http://www.angewandte.com> or from the author.

formational restraints, bicyclic *cis*-peptidyl proline surrogates were investigated with low yielding and nonselective multi-step reaction sequences.^[4, 5] Stimulated by a recently described Molecular Dynamic (MD) study,^[6] we herein present the design of a lactam-bridged type VIa β -turn mimetic (**1**). NMR spectroscopy based conformational analysis and a practical and efficient EPC synthesis of a model peptide surrogate by the self-reproduction of chirality methodology of Seebach et al.^[7] and Grubbs' ring-closing olefin metathesis (RCM)^[8] are also reported (Scheme 1).



Scheme 1.

Following the above strategy, we approached to the α -alkylproline derivative **3** by employing the concept of self-reproduction of chirality^[7] which was recently re-investigated by Wang and Germanas^[9] (Scheme 2). Thus, diastereocon-

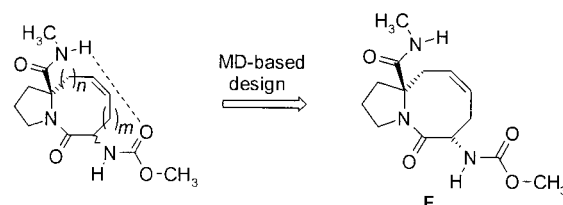


Scheme 2. a) $\text{CCl}_3\text{CH}(\text{OH})_2$, C_6H_6 , 80°C ; b) lithium diisopropylamide (LDA), allyl bromide, THF, -78°C ; c) HCl, MeOH, NaHCO_3 ; d) **5a**: $\text{X} = \text{Cl}$, $n = 0$, CH_2Cl_2 , NEt_3 , $0^\circ\text{C} \rightarrow \text{RT}$, **5b**: $\text{X} = \text{OH}$, $n = 1$, **5c**: $\text{X} = \text{OH}$, $n = 2$, 4-methyl morpholine (NMM), ClCO_2tBu , THF; e) $[\text{Ru}]$, CH_2Cl_2 (Cy = cyclohexyl).

trolled C-alkylation of the bicyclic proline derivative **2a** furnished the N,O-acetal **2b** which was transformed into α -allylproline ester **3** by treatment with one equivalent of HCl in methanol. To evaluate the scope of our synthetic concept, we tried to prepare differently sized bicyclic model lactams of type **4**. Thus, the RCM precursors **5a–c** were synthesized by N-acylation of the proline derivative **3**. The subsequent RCM experiments were performed using the ruthenium-based catalyst **I**^[10] in refluxing CH_2Cl_2 which proved to be the solvent of choice. The dienes **5a, b** underwent clean conversion to furnish the 5,6- and 5,7-fused unsaturated bicyclic lactams **4a, b** in 91 and 75 % yield, respectively. To minimize competing intermolecular oligomerization processes,^[11] a high

dilution technique was employed for the conversion of the diene **5c** into the bicyclic azocine **4c**. 10 mol % of the catalyst was chosen to initiate the metathesis reaction and a second portion of catalyst^[12] (2 mol %) was added after 24 h. Gratifyingly, the desired cyclization took place without any detectable oligomerization products, although complete conversion could not be achieved.

To decide which ring size and configuration is most promising in terms of possible intramolecular hydrogen-bond interactions, we performed MD simulations on the different target structures **A–F** shown in Scheme 3. All calculations



Formula	<i>n</i>	<i>m</i>	Stereochemistry
A	0	0	<i>cis</i>
B	0	0	<i>trans</i>
C	1	0	<i>cis</i>
D	1	0	<i>trans</i>
E	1	1	<i>cis</i>
F	1	1	<i>trans</i>

Scheme 3.

were performed in the gas phase with no continuum model or explicit solvent molecules present, using the AM1 Hamiltonian implemented in the semiempirical program package VAMP7.0.^[13] After heating the system to 400 K, 1200 geometries were sampled at constant temperature resulting in a total data-acquisition time of 120 ps. The integration time step was 1 fs, the coupling constant to the heat bath 40 fs. The ability to form a hydrogen bond was rated by a time-dependent plot of the two possible donor–acceptor interactions, which lead either to a type VIa, or, by reorientation of the C- and N-termini by rotation about the torsion angles Ψ_3 and Φ_2 (see Scheme 1), respectively, to a type VIb turn, which involve CO^{i+2} and NH^{i+1} . Classification of the β -turn type was done by time-dependent analysis of the dihedral angles Ψ_3 and Φ_2 , in accord with the data published by Robinson.^[14]

For the six-membered lactams, the *cis*-isomer **A** allows the formation of both possible hydrogen bonds. However, for the chosen simulation conditions, no distinct turn pattern can be assigned. For the *trans*-isomer **B**, the formation of a hydrogen bond is geometrically not possible. Expanding the ring by one methylene unit leads to the fused azacycloheptenones **C** and **D**. According to the MD simulations, the increased flexibility resulted in a growing tendency of the *trans*-isomer **D** to form a type VIa2 interaction pattern. Nevertheless, the mean $\text{NH} \cdots \text{OC}$ distance of 4.6 Å is too large for a stable hydrogen bond. Similar to **A**, the homologue **C** is able to form both hydrogen-bonding interactions. During the simulations, a type VIa1 pattern was established several times, but, in spite of the corresponding hydrogen-bond interaction, no typical VIb motif was observed. The fused eight-membered lactams **E** and

F exhibited the most interesting behavior. For the *cis*-isomer **E** a hydrogen bond between the amide carbonyl and the carbamate NH was observed, however, the flexibility within the molecule allowed switching to a type VIa-like hydrogen-bond interaction (this occurred several times during the simulation). Moreover, the *trans*-isomer **F** formed only one hydrogen-bonding pattern, a type VIa2 subtype ($\Psi_3 = 0^\circ$ and $\Phi_2 = -120^\circ$) of the β -VI turn family (Figure 1a). As a

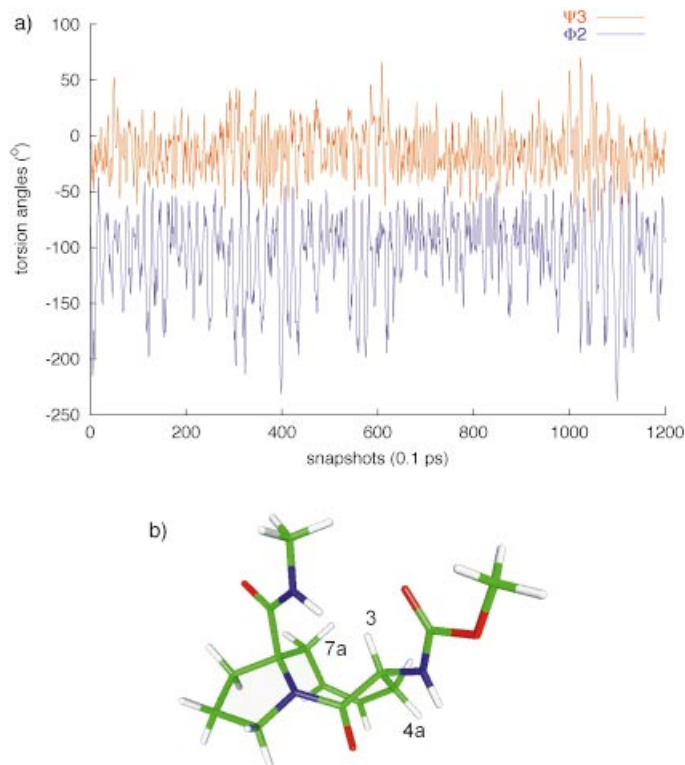


Figure 1. a) Plot of the dihedral angles Ψ_3 and Φ_2 calculated from the 120 ps semiempirical MD simulation (AM1, 400 K) of compound **F**. Note that the mean values come close to the ideal angles of a type VIa2 turn ($\Psi_3 = 0^\circ$ and $\Phi_2 = -120^\circ$).^[14] No conformational interchange can be observed. b) Representative example of a conformation extracted from the trajectory. The dihedral angles $\Psi_3 = 23^\circ$ and $\Phi_2 = -102^\circ$ result in a $\text{NH} \cdots \text{OC}$ distance of 2.3 Å for this non-equilibrium conformation.

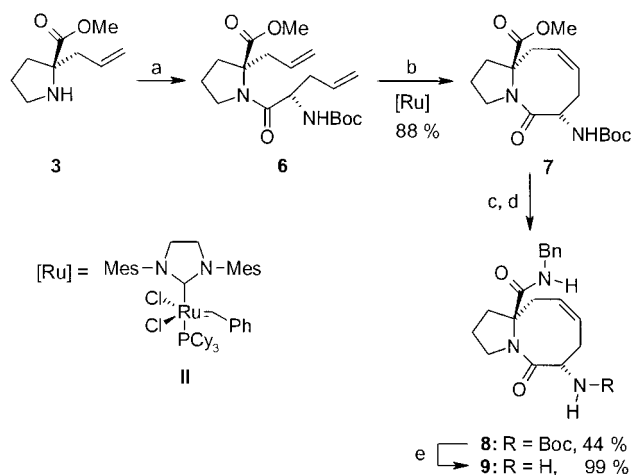
representative geometrical example, a snapshot taken from the MD simulation of compound **F** is shown (Figure 1b). The conformational behavior is independent from the starting geometry of the simulation. Beginning with a geometry-optimized type VIb turn, the conformation of the molecule switches to a stable VIa2 motif after a few picoseconds of data acquisition.

Comparison of all six simulations strongly supports the assumption that the lactam-bridged peptide surrogate **F** should be most suitable for the formation of a hydrogen-bonding pattern leading to a successful type VIa β -turn mimetic.

To account for solvent effects which may influence the conformational preferences of peptide-like structures, we repeated the calculations applying the COSMO approach of Klamt and Schüürmann.^[15] This technique describes quantum mechanically the macroscopic environment by polarization

charges at the boundary between the solute and the continuum (water, dielectric constant = 78.4) and therefore represents the dielectric properties of the bulk molecules. Both series of simulations show the same principal behavior. As a general effect, structural fluctuations are damped by the environment, which leads to a more meaningful interpretation of the data.

To experimentally verify our MD simulation prediction of type VIa β -turn inducing properties for the bicyclic peptidomimetic **F**, the RCM precursor **6** was prepared starting from *tert*-butoxycarbonyl (Boc) protected (*S*)-allylglycine and the α -allylproline **3** (Scheme 4). Subsequently, Ru-catalyzed ring-closure of the protected dipeptide **6** led to formation of the



Scheme 4. a) (*S*)-*N*-Boc-2-amino-4-pentenoic acid, NMM, ClCO_2tBu , THF; b) 7 mol % [Ru], CH_2Cl_2 , 40°C ; c) LiOH, dioxane/ H_2O ; d) BnNH_2 (Bn = benzyl), *N,N'*-dicyclohexyl carbodiimide (DCC), CH_2Cl_2 , 1-hydroxy-1*H*-benzotriazole (HOBt); e) HCl/diethyl ether.

eight-membered azacycle **7** in 57% yield. To improve the efficiency of the reaction we tried the highly active N-heterocyclic carbene-coordinated catalyst **II**.^[16] Actually, the metathesis reaction proceeded smoothly with only 7 mol % of catalyst to yield the bicyclic olefin **7** in 88% (12 h, reflux). Finally, hydrolysis of the ester function and DCC coupling to benzylamine as a representative NH-providing unit gave the target model peptide **8** that could be readily transformed into the primary amine **9**.

Conformational analysis of the lactam-bridged peptidomimetic **8** is mainly based on NMR spectroscopy, particularly on coupling constants, NOEs, and variable temperature (VT) measurements. A strong NOE was detected between H-7a and H-3 indicating the transannular proximity of these two protons in a boat conformation of the eight-membered lactam ring. In combination with a detailed analysis of the proton couplings further strong NOEs between the amide N-H and H-3 and the carbamate N-H and H-4a, respectively, were diagnostic for a type VIa β -turn conformation adopted by the lactam **8**. Clearly the fused ring system is fixed in a stable conformation which forces the substituents at C-3 and C-8 into an orientation able to form a hydrogen bond between the amide NH and the carbamate C=O as predicted by the MD calculations. The presence of an intramolecular hydrogen

bond, indicated by the comparatively downfield shift ($\delta = 8.11$) of the amide N–H resonance was unambiguously demonstrated by comparison of the amide N–H shifts in the spectra (in CDCl_3) of the carbamate **8** and the amine **9** when the signal of the amide N–H appeared significantly shifted upfield ($\Delta\delta = 1.61$) after removal of the Boc unit. Besides the main conformational population, VT NMR experiments which showed a significant chemical-shift change ($\Delta\delta/\Delta T = -5.2 \text{ ppb K}^{-1}$) gave evidence for a temperature dependant coexistence of non-hydrogen bonded conformations,^[17] corroborated by NOEs between H-3 and the carbamate N–H at elevated temperature (330 K, CDCl_3). The FT-infrared (IR) spectrum displayed an extensive absorption at 3350 cm^{-1} characteristic for a hydrogen bonded amide and an absorption at 3405 cm^{-1} also indicating the coexistence of a solvent-exposed amide.

In conclusion, a highly efficient proline-based type VI β -turn mimetic was designed employing the results of molecular dynamics simulation. EPC synthesis involving Seebach's self-reproduction of chirality methodology and Grubbs' ring-closing olefin metathesis gave access to the novel molecular scaffold.

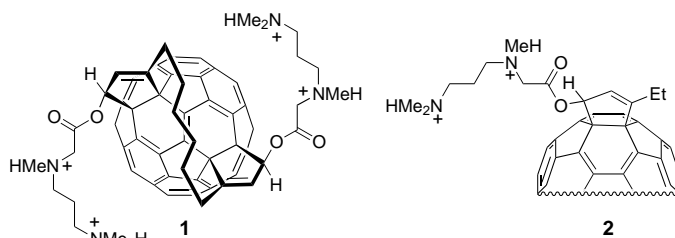
Received: March 12, 2001
Revised: June 26, 2001 [Z16752]

- [1] M. S. P. Sansom, H. Weinstein, *Trends Pharmacol. Sci.* **2000**, *21*, 445–451.
- [2] S. Fischer, R. L. Dunbrack, Jr., M. Karplus, *J. Am. Chem. Soc.* **1994**, *116*, 11931–11937.
- [3] A. Wittelsberger, M. Keller, L. Scarpellino, L. Patiny, H. Acha-Orbea, M. Mutter, *Angew. Chem.* **2000**, *112*, 1153–1156; *Angew. Chem. Int. Ed.* **2000**, *39*, 1111–1115.
- [4] D. Gramberg, C. Weber, R. Beeli, J. Inglis, C. Bruns, J. A. Robinson, *Helv. Chim. Acta* **1995**, *78*, 1588–1606.
- [5] K. Kim, J. P. Germanas, *J. Org. Chem.* **1997**, *62*, 2847–2852.
- [6] G. Müller, G. Hessler, H. Y. Decornez, *Angew. Chem.* **2000**, *112*, 926–928; *Angew. Chem. Int. Ed.* **2000**, *39*, 894–896.
- [7] D. Seebach, M. Boes, R. Naef, W. B. Schweizer, *J. Am. Chem. Soc.* **1983**, *105*, 5390–5398.
- [8] a) R. H. Grubbs, S. Chang, *Tetrahedron* **1998**, *54*, 4413–4450; b) M. Schuster, S. Blechert, *Angew. Chem.* **1997**, *109*, 2124–2144; *Angew. Chem. Int. Ed. Engl.* **1997**, *36*, 2036–2055; c) A. Fürstner, *Angew. Chem.* **2000**, *112*, 3140–3172; *Angew. Chem. Int. Ed.* **2000**, *39*, 3012–3043.
- [9] H. Wang, J. P. Germanas, *Synlett* **1999**, *7*, 33–36.
- [10] P. Schwab, R. H. Grubbs, J. W. Ziller, *J. Am. Chem. Soc.* **1996**, *118*, 100–110.
- [11] a) "Alkene Metathesis in Organic Synthesis": A. Fürstner, *Top. Organomet. Chem.* **1998**, *1*, 37–72; b) E. L. Dias, S. T. Nguyen, R. H. Grubbs, *J. Am. Chem. Soc.* **1997**, *118*, 3887–3897.
- [12] M. Ulman, R. H. Grubbs, *J. Org. Chem.* **1999**, *64*, 7202–7207.
- [13] T. Clark, A. Alex, B. Beck, J. Chandrasekar, P. Gedeck, A. Horn, M. Hutter, B. Martin, G. Rauhut, W. Sauer, T. Schindler, T. Steinke, *Programme Package VAMP7.0*, Oxford Molecular Group Plc., Oxford, **1998**.
- [14] J. A. Robinson, *Synlett* **2000**, *4*, 429–441.
- [15] A. Klamt, G. Schüürmann, *J. Chem. Soc. Perkin Trans. 2* **1993**, 799–805.
- [16] M. Scholl, S. Ding, C. W. Lee, R. H. Grubbs, *Org. Lett.* **1999**, *1*, 953–956.
- [17] a) L. Belvisi, C. Gennari, A. Mielgo, D. Potenza, C. Scolastico, *Eur. J. Org. Chem.* **1999**, 389–400; b) E. S. Stevens, N. Sugawara, C. M. Bonora, C. Toniolo, *J. Am. Chem. Soc.* **1980**, *102*, 7048–7050; c) K. Weber, U. Ohnmacht, P. Gmeiner, *J. Org. Chem.* **2000**, *65*, 7406–7416.

Atomic Force Microscope Studies on Condensation of Plasmid DNA with Functionalized Fullerenes**

Hiroyuki Isobe, Sho Sugiyama, Ken-ichi Fukui, Yasuhiro Iwasawa, and Eiichi Nakamura*

A recent paper reported the first example of the use of a carbon cluster as a vector to deliver DNA into mammalian cells.^[1, 2] Thus, mixed with the tailor-made tetraminofullerene **1**, a plasmid DNA forms micrometer-sized fullerene–DNA particles as observed by optical microscope, which, after



incubation with the target cells, became located inside the cytoplasm as phagocytes. Expression of the encoded gene took place over several days, indicating that the plasmid DNA was released into the cytoplasm without being damaged by the fullerene complexation. Although these biological experiments demonstrated the ability of the fullerene **1** to condense and release DNA, the molecular nature of such reversible DNA condensation remained unclear. We report herein the results of atomic force microscope (AFM) studies^[3] that provided molecular-level information on the DNA condensation/release processes induced by fullerene vesicles.^[4] When used in a small quantity, the fullerene **1** condenses a single plasmid DNA into a **1**–DNA complex. Upon further addition of **1**, many single-molecule DNA condensates gather together to form the micrometer-sized fullerene–DNA particles observed previously by optical microscopy. Release of the DNA molecules from these large particles was achieved experimentally by removal of the fullerene through CHCl_3 extraction.

The interactions between the fullerene **1** and DNA were probed for 4 kbp supercoiled plasmid DNA (pBR322). Thus, we added an increasing amount of **1** to a pH 7.6 buffer solution of pBR322 and plotted the amount of the DNA mobile on the gel against the reagent/base pair ratio (R). As shown in Figure 1 (solid line), there was observed precipitous decrease

[*] Prof. Dr. E. Nakamura, Dr. H. Isobe, S. Sugiyama, Dr. K.-i. Fukui, Prof. Dr. Y. Iwasawa
Department of Chemistry
The University of Tokyo
Hongo, Bunkyo-ku, Tokyo 113-0033 (Japan)
Fax: (+81) 3-5800-6889
E-mail: nakamura@chem.s.u-tokyo.ac.jp

[**] This research was supported by Grant-in-Aid for Specially Promoted Research from Ministry of Education, Culture, Sports, Science, and Technology.

Supporting information for this article is available on the WWW under <http://www.angewandte.com> or from the author.